Comparison of microcrack formation boundaries determined by complex of physical methods with long-term strength of expanded clay concrete under different types of stress state

Chorikul Raupov* and *Ganisher* Malikov

Tashkent State Transport University, Tashkent, 100067, Uzbekistan

Abstract. This work aims to experimentally study the strength and strain of expanded clay concrete during short-term and long-term compression and tension under various loading modes.
A technique for testing expanded clay concrete under short-term and long-term compression and tension, including the boundaries of microcrack formation by a complex of physical methods (tensometric, ultrasonic pulsed, and acoustic emission), is given.
The results of tests of expanded clay concrete under short-term and long-term monotonic loading under compression and tension and low-cycle loading under compression, as well as the boundaries of microcrack formation by a complex of physical methods, are obtained. The boundaries of microcrack formation are compared with the long-term strength of expanded clay concrete under various types of stressed states. Strain diagrams of expanded clay concrete under axial compression and tension, and "ultrasound transmission speed - stress level" and "number of acoustic pulses - stress level" diagrams are also obtained.
Empirical formulas are proposed for determining the boundaries of microcracking in expanded clay concrete and the relationship between the level of long-term strength and the time of staying specimens under load in compression and tension. The results allow the formulation of several proposals and clarifications for normative documents to calculate and design lightweight concrete elements and structures.

1 Introduction

The widespread use of local artificial porous aggregates instead of natural heavy aggregates in seismic regions of the Republic of Uzbekistan with a dry, hot climate is a governing condition for increasing the efficiency of capital investments in the construction of transport and other important structures. A distinctive feature of expanded clay, which in terms of producing lightweight concrete from porous aggregates, ranks first in comparison with other porous aggregates, is its relatively high strength at a relatively lower bulk

*Corresponding author: raupovch@gmail.com

density. Expanded clay concrete in bridge building instead of traditional concrete can significantly reduce the weight of structures, material consumption, transport and installation costs, and labor costs while maintaining the necessary strength, reliability, and durability of structures. It can improve performance, reduce loads on foundations, reduce the cost of bridge construction and, at the same time, speed up their construction [1 – 7].

Theories of strength and fracture under compression and tension are of great importance for predicting the physical and mechanical characteristics of concrete, in particular, the concepts of the boundaries of microcracking (R^o_{crc} and R^v_{crc}) [3, 8 – 15] and long-term strength (R_{bl} and R_{btl}) [2, 3, 16, 17]. With these theories, it is possible to assess the kinetics of the process of microcracking in concrete and the safety margins of structures. The boundaries of microcracking and long-term compressive and tensile strength should be considered important characteristics of concrete to ensure reliable operation of the structure. The values of the boundaries of microcrack formation are quite important for describing the features of concrete behavior since they allow concluding the stage of the stress-strain state (SSS) [9].

An analysis of the results of studies on the boundaries of microcrack formation shows that these characteristics are ambiguously related to the compressive strength R_b and can vary significantly depending on the proportion of expanded clay concrete mix, the type and consumption of coarse aggregate, and other factors [3, 8–14].

Particular attention is paid to the upper limit of microcrack formation since reaching this boundary indicates the transition to the third stage of the SSS, i.e., this indicates that microcracks merge into macrocracks and divide the concrete structure into blocks. The blocks under load are displaced relative to each other, which causes the concrete matrix destruction [9-12]. If the load level is close to the upper limit of microcracking but does not exceed it, plastic strains under static loading stabilize over time (even under cyclic changes of loading [18, 19]). At present, the derivation of new formulas (more universal ones) applicable to concretes of different types and classes is relevant.

The opinions of researchers in determining the relative limit of long-term strength differ, as evidenced by the data given in [2, 3, 15, 16].

In recent years, several formulas have been proposed that allow a more differentiated approach to assessing the relative limit of the long-term strength of concrete. Therefore, for heavy concretes of ordinary classes, used earlier, good results are given by the following formula [16]

$$R_{bl}/R_b = 0.92 - 0.4\lg(t - \tau_1) \qquad (1)$$

where τ_1 is the age of concrete at the time of loading.

For heavy concrete of class B30 and higher at an old age, the following dependence can be used:

$$R_{bl}/R_b = 0.35\lg R_b + 0.175) \qquad (2)$$

If the concrete of the same classes is loaded at middle age, when the hardening processes continue to influence parameter R, then the long-term strength can be determined by the following formula

$$R_{bl} = R^o_{crc} + 0.4R_b. \qquad (3)$$

Since the parameters depend mainly on the class of concrete, its age at the time of loading, the gain in strength, and the conditions of moisture exchange with the surrounding medium, it can be assumed that the ultimate strength depends mainly on the same factors.

However, several issues related to the study of lightweight concrete elements and structures, including their operation under various stress states and loading modes, have not yet been studied or are insufficiently studied. The proposed article presents the main results of these studies, which allow us to formulate several proposals and specifications for regulatory documents on the calculation and design of lightweight concrete elements and structures.

2 Methods

The composition and main characteristics of concrete are given in Tables 1 and 2. Expanded clay gravel of two fractions, 5–10 and 10–20 mm in a ratio of 40:60, was taken as a coarse aggregate produced in the Tashkent cement plant. As Portland cement, the cement of the Navoi cement plant was used, and the sand of the Tashkent quarry was used as quartz sand.

Table 1. Composition of expanded clay concrete (EC)

Actual consumption of materials per m^3 of concrete	Cement, kg	427
	sand, kg	629
	expanded clay, kg (l)	414 (727)
W/C (water/cement ratio)		0.49

Table 2. Characteristics of expanded clay concrete

Bulk density of dry expanded clay concrete, kg/m^3	1760
Cubic strength, R, MPa	33.0
Prism strength, R_b, MPa	28.4
Prism strength factor, R_b/R	0.86
Initial modulus of elasticity, E_b, Pa	15.4

Note: Specimens were tested at the age of 28 days. Prisms dimensions - 150x150x600 mm, cubes ribs - 150 mm. The cone slump of concrete mix - 1...2 cm.

2.1 The procedure for testing expanded clay concrete during short-term testing; measuring instruments

Monotonic loading under compression and tension. Loading of specimens (prisms) of 70x70x280 mm and 150x150x600 mm dimensions and cylinders of 70 mm in diameter and 235 mm in height, made of expanded clay concrete under short-term compression and tension, was performed according to the standard procedure on testing machines UMM-20 and P-250 with a maximum capacity of 200 and 2500 kN, respectively. Specimen loading was conducted in steps of no more than 0.1 of the expected breaking load with staying on the steps until the increase in short-term creep deformations ceased. The duration of staying on the steps under stepwise compression loading of specimens did not exceed 5 min.

Low-cycle loading under compression. Some specimens were tested under cyclic loading. Each step contained 1 cycle of loading and destruction. The duration of load staying at the upper and lower stress levels of a given step was determined by reaching such a shape of the deformation diagram when, within the measurement accuracy, the hysteresis loop ceased to increase. This loading pattern was realized up to a stress level not exceeding the upper limit of microcrack formation [20, 21].

During short-term tests, longitudinal and transverse strains were measured with wiring strain paper gauges of the CNIISK experimental mechanical plant with their bases of 20 and 50 mm.

To obtain information about the integral value of strains, longitudinal and transverse strains were measured in several sections along the length of the specimen, covering a certain volume of material [5]. The adopted pattern of strain gauge gluing is shown in Figures. 1 *a, b, c*. The dimensions of the tested prisms and the base of strain gauges determined the use of each pattern. Strain gauges were glued according to the standard method - three months before the start of the test. The scheme of prisms and cylinders installation in a testing machine is shown in Figure 2.

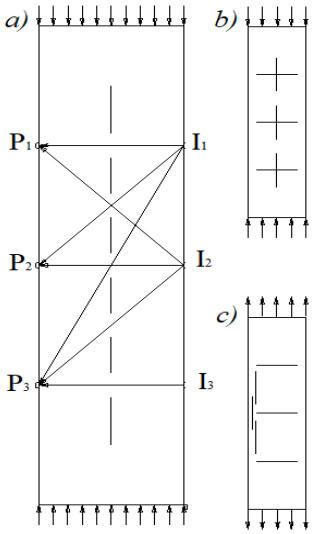

Fig. 1. Scheme of ultrasonic and tensometric measurements

Under compression tests, the specimens were centered along the physical axis by trial loading of no more than $0.20R_b$ (Figure 2, *a*). Under tensile testing, the load on the specimen was transferred through Hooke's hinges using collet grippers, ensuring uniform strain distribution along the specimen's length and reliable transfer of axial tensile force to the specimen. (Figure 2, *b*).

a) *b)*

Fig. 2. Testing specimens under short-term compression (a) and tension (b)

2.2 The procedure for testing expanded clay concrete during long-term testing; measuring instruments

Long-term loading of specimens to a given level of stresses under compression and tension was conducted in spring and lever installations with a maximum force of 210 kN and 30 kN, respectively.

One or two specimens were placed in the installation. The first scheme was used under high loading levels (Figure 3, a), and the second was used under low loading levels (Figure 3, *b*).

Metal plates 20 mm thick were laid between them when installing two prisms, and when installing two cylinders, a Hooke hinge was laid (Figure 3, *c*). The value of the load was set according to the range of springs, pre-calibrated on the press, on which the short-term loading was performed.

Under tensile tests, the cylinders were placed in the installation using collets and Hooke's hinges, and under compression tests, the prisms were installed with metal base plates 30 cm thick with ball joints glued to the ends.

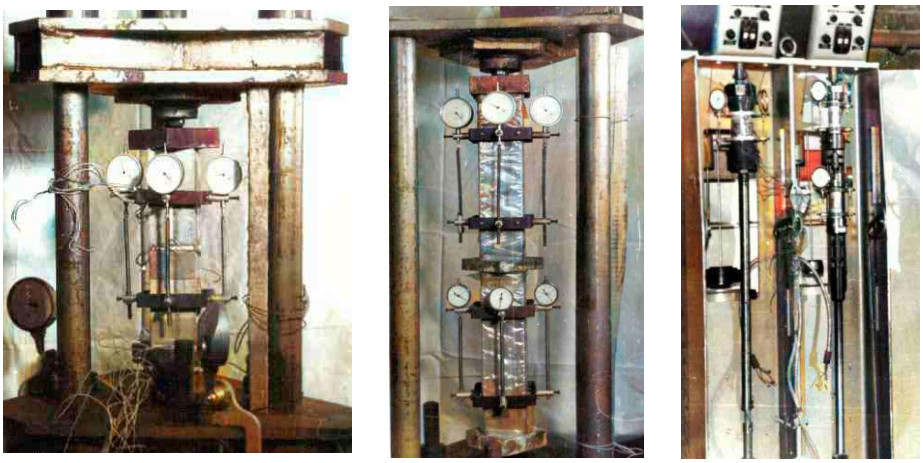

a) *b)* *c)*

Fig. 3. Testing of specimens under long-term compression (a, b) and tension (c).

The range of springs during calibration was measured with PAO-6 deflection meters with a division value of 0.01 mm, installed on two opposite sides (generatrices) of springs.

To eliminate the error related to non-additivity of shrinkage and creep, the specimens before loading were waterproofed from the sides with a layer of paraffin 2–3 mm thick and two layers of polyethylene film with seams glued by insulating tape.

2.3 Short-term strength of expanded clay concrete under axial compression and tension

Monotonic compression and tension loading. The strength and strain characteristics of expanded clay concrete under compression and tension are summarized in Tables 3 and 4.

Table 3. Results of short-term axial compression tests

Characteristics	Values
Cubic strength of expanded clay concrete, R, at the age of 220, 530, and 800 days, respectively, MPa	36.5, 43.5 and 48.2
Prism strength, R_b, at the age of 220, 530, and 800 days, respectively, MPa	34.3, 37.4 and 35.7
Prism strength factor, R_b/R	0.94, 0.86 and 0.74
R_b/R, at the age of 220, 530, and 800 days, respectively	0.94, 0.96 and 0.74
Modulus of elasticity, E_b, at the age of 220, 530, and 800 days, respectively, GPa	18.7, 22.0 and 22.9
Poisson's ratio, ν_e, at the age of 220, 530, and 800 days, respectively	0.20, 0.19 and 0.20
Compressibility at $0.95R_b$ $\varepsilon_{x(\sigma=0.95Rb)}.10^{-5}$, at the age of 220, 530 and 800 days, respectively	192, 181 and 168

Note: Results for expanded clay concrete at the age of 220 and 530 days were obtained for specimens 70x70x280 mm, at the age of 800 days - for specimens 150x150x600 mm.

Table 4. Results of short-term axial tensile tests

Characteristics	Values
Tensile strength, R_{bt}, at the age of 220 and 530 days, respectively, MPa	2.06 and 2.30
Modulus of elasticity, E_b, at the age of 220 and 530 days, respectively, GPa;	23.3 and 23.5
Poisson's ratio, ν_e, at the age of 220 and 530 days, respectively	0.20 and 0.20
Tensile strength at $0.95R_{bt}$ $\varepsilon_{x(\sigma=0.95Rb)}.10^{-5}$, at the age of 220 and 530 days, respectively	10 and 10

The data obtained (Table 3) on the increase in time of cubic R and prism R_b strength of expanded clay concrete confirmed that the measures we took to protect specimens from drying out during storage were sufficient, and they provided a normal hardening condition for 800 days, which is very important when comparing the results of short-term and long-term tests.

The increase in the elasticity modulus of expanded clay concrete under compression over time by the end of the experiment (τ_1= 800 days) was 30-50% higher than at the age of τ_1=28 days (Tables 2 and 3). The increase in the tensile modulus was less significant. So, by τ_1= 530 days, it increased only by 5% compared to τ_1= 220 days, while under compression over this time interval, the value of E_b increased by 15%.

For expanded clay concrete, the values of R_b/R exceed the ones specified in the existing standards for traditional concrete. Other researchers noted the increased prismatic strength of expanded clay concrete as well [1-5, 9-13]. They explained that porous aggregates have a more developed surface and better adhesion with the cement-sand component than dense aggregates. This largely restrains the transverse deformations of the prisms. However, with an increase in age, there was a noticeable decrease in the prism strength coefficient of expanded clay concrete (Table 3), and at the age of 800 days, R_b/R was 88% of R_b/R at 28 days of age (Table 2).

According to our experimental data, the coefficient of variation for the strength and strain properties of expanded clay concrete under compression and tension was 1–6% and 3–14%, respectively.

High values of the coefficients of variation under tension obtained in the experiments are due to two factors associated with the different nature of concrete destruction under compression and tension, respectively, and with different relative accuracy of

measurements. Under axial tension, the destruction of the sample passes along one section due to a local defect in the macrostructure. As experiments have shown [5], there is practically no redistribution of stresses and strains between sections in concrete, and a weak section determines the strength of the entire sample.

Under compression, the effect of strain and stress localization is less pronounced due to their partial distribution over the entire volume of the specimen. The relative accuracy of measurements under compression and tension is because the values of stress and strain measured during tensile testing are an order of magnitude less than under compression, while the resolution of force gauges and especially strain gauges is the same. This factor is especially pronounced when measuring tensile strains since their measurement accuracy, which does not exceed 1(10–5, is commensurate with the measured strains, especially at low loading levels.

The ratio of compressive and tensile strengths. The results of determining the axial tensile strength R_{bt} were compared with the results obtained for the cubic strength R and prism strength R_b (Tables 1–3).

In our experiments, the R_{bt}/R ratio was 0.05...0.06, and R_{bt}/R_b was 0.06...0.07. The high ratio of R_{bt}/R for expanded clay concrete in our experiments is explained by the test procedure, where practical axial tension was ensured under the testing of cylinders. In addition, tensile tests of cylinders show better results than prisms due to the smaller effect of friction in the corners of the specimen. The ratio of R_{bt}/R for expanded clay concrete can be approximately taken equal to 0.05.

Low-cycle compressive loading. The test results under low-cycle compressive loading are summarized in Table 5. A comparison of the data obtained with the data given in Tables 2 and 3 showed that low-cycle loading under compression did not affect the strength of expanded clay concrete and mixes (the difference between the values of R_b did not exceed 6%).

Table 5. Test results under low-cycle compressive loading

Prism strength R_b, MPa		35.1
Modulus of elasticity E_b, GPa at the loading cycle	The first	19.7
	The last	19.0
Initial Poisson's ratio ν_e at the loading cycle	The first	0.21
	The last	0.22

The results indicate the best resistance of expanded clay concrete under low-cycle compressive loading and the expediency of their use in transport engineering, where the structure is subject to multiple low-cycle loads. The values of Poisson's ratio ν_e practically did not change and did not differ from those obtained under monotonic loading. The elasticity modulus E_b of expanded clay concrete decreased by the last cycle by approximately 4%.

3 Results and Discussion

3.1 Determination of the boundaries of micro-crack formation in expanded clay concrete by a complex of physical methods

Tensometric method. Determination of R^o_{crc} and R^v_{crc} by tensometric methods based on the analysis of experimental $''\eta–\varepsilon''$ diagrams was performed according to the method described in [15] by measuring longitudinal and transverse strains under loading.

Figures 4 and 5 show averaged diagrams of expanded clay concrete deformation

obtained when testing specimens under compression and tension. Visually, general patterns of the deformation diagrams under axial compression and tension are similar. However, in the case of compression, the nonlinearity of the diagrams manifested itself earlier, and the degree of its curvature was greater than in the case of tension. A characteristic feature of all strain diagrams was an almost linear dependence between stresses and strains over a large part of the stress range. Inelastic strains were noted only at loading levels greater than 0.70.

Based on the measurement results, the average values of the longitudinal ε_x and transverse ε_y strains of the specimen were calculated, and, on their basis, volumetric strain ε_v, its increment $\Delta\varepsilon_v$, and the differential coefficient of transverse strain were determined at each stage of loading. The graphs of changes in these characteristics (Figure 4) were plotted depending on the relative level of loading. Five prisms were tested for expanded clay concrete. The values of mechanical characteristics (prism strength, modulus of elasticity, Poisson's ratio) were determined as an average of data for five specimens.

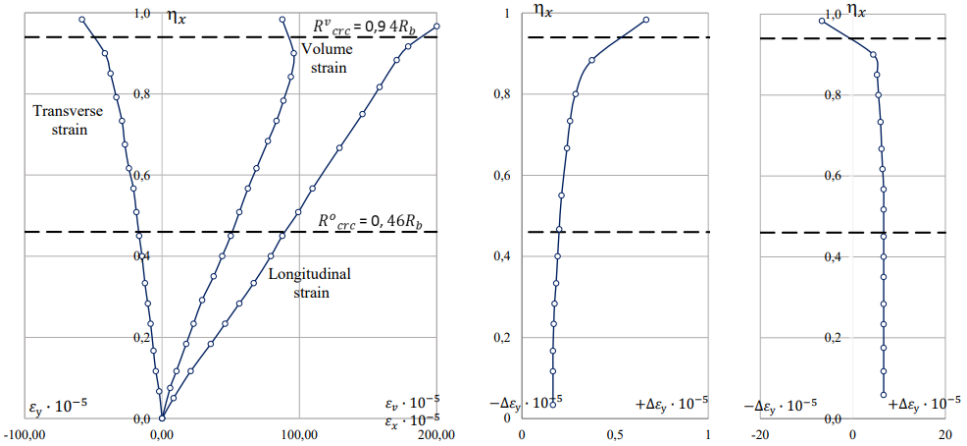

Fig. 4. Strain of expanded clay concrete under axial compression (prism dimensions 70x70x280 mm)

A comparison of the strains determined by individual strain gauges on the specimen showed that the spread of their values was relatively small and changed little as the load increased. The coefficient of variation of readings from longitudinal strain gauges glued on different faces of the prism did not exceed 10%. This scatter was mainly because the actual axis of load application did not coincide with the physical axis of the specimen. In comparing the readings from strain gauges located in different sections along the height on the same face, their coefficient of variation did not exceed 5%. Considering these results, the strains were determined as the arithmetic average values according to the readings of all strain gauges.

A comparison of the values of transverse strains, determined by individual strain gauges on the specimen, showed that they were characterized not only by a higher spread (the coefficient of variation of their values was up to 40%) but by a sharp difference in the readings of individual strain gauges at individual points on the surface of the specimen (in the zone of potential destructions) almost from the beginning of loading. From experimental diagrams, strain values at 0.95 of breaking load were determined since data on the compressibility and extensibility of concrete are used to solve several issues in the design and evaluation of research results. For expanded clay concrete and heavy concrete, compressibility depends on several factors, of which the most important are the strength of concrete, the material of the aggregate, and the stress level of concrete [2, 6, 17].

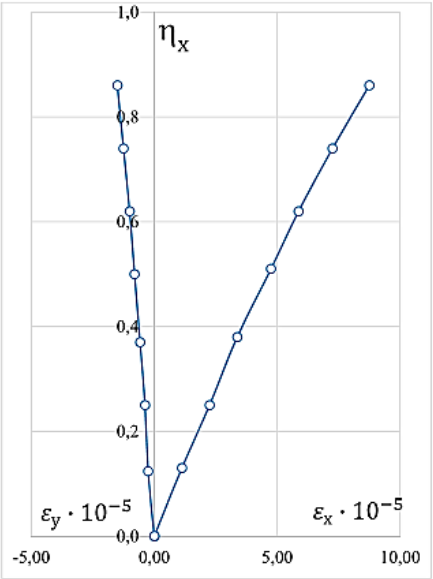

Fig. 5. Strain of expanded clay concrete under axial tension

Ultrasonic pulse method. The average diagrams of the change in the velocity of transmission of the generated ultrasonic pulses through the specimen are shown in Figures 6 and 7, and the results of determining R^0_{crc} are given in Table 6. Here, as well as in the case of the tensometric measurement method, the values of R^0_{crc}, determined from different scanning traces, can differ from each other by 20%.

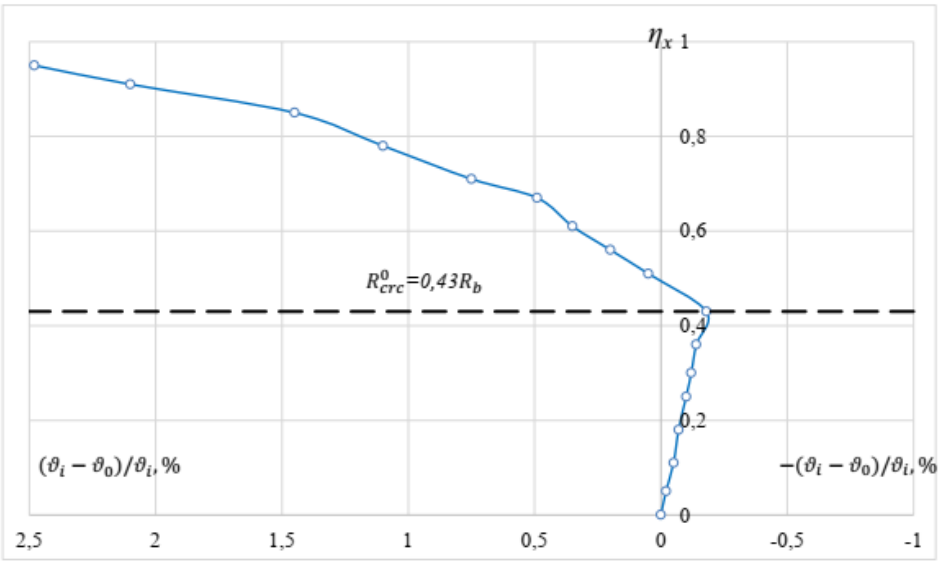

Fig. 6. Diagram "velocity of ultrasound transmission vs. stress level in expanded clay concrete specimens"

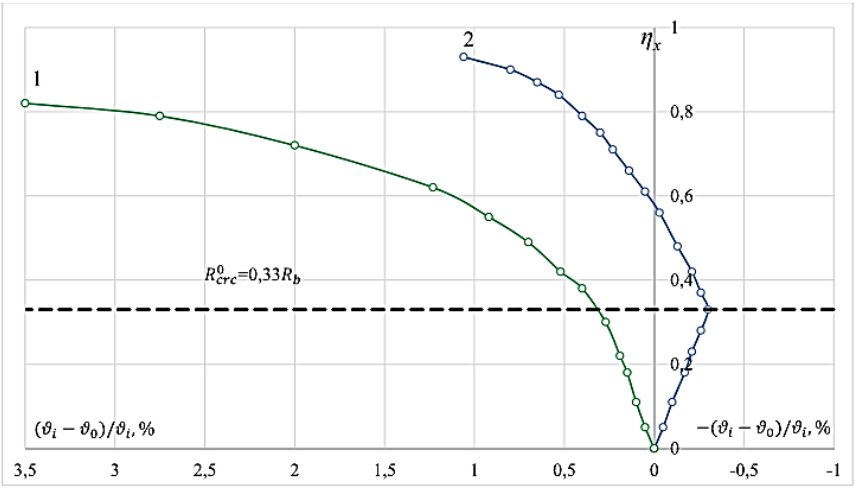

Fig. 7. Diagram "velocity of ultrasound transmission vs. stress level in expanded clay concrete specimens" at perpendicular (1) and diagonal (2) scanning

Acoustic emission method. The experiments show (Figure 8) that the acoustic pulses accompanying the destruction of concrete structures are recorded almost from the moment of application of the compressive load and have several intensity peaks during the loading process. A point on the "$\eta - N$" diagram before the beginning of the first peak of the intensity of the growth of impulses N is taken as the lower boundary of microcracks, and a point before the last peak is taken as the upper boundary of microcracks. The first peak corresponds to the microcrack development scheme proposed in [3, 15], to the formation of a system of microcracks originating from the initial cracks on the grains of the coarse aggregate. The next possible peaks should correspond to the formation of local systems of intergrown microcracks, and the subsequent peak should correspond to the formation of main macrocracks of destruction. The values of R^0_{crc}, obtained by the acoustic emission method (Table 6) are in good agreement with the values of R^v_{crc}, obtained by the tensometric method in the fracture zone (the discrepancy is no more than 8%).

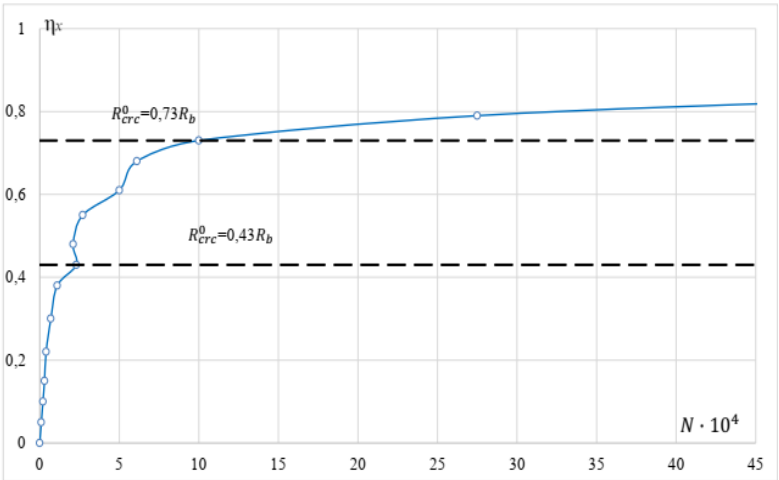

Fig. 8. Diagram "number of acoustic pulses vs. stress level in expanded clay concrete specimens"

The results of determining the boundaries of microcrack formation R^0_{crc}/R_b and R^v_{crc}/R_b by a complex of physical methods (strain gauge, ultrasonic pulse, and acoustic emission method) are given in Table 6.

Table 6. Results of determining the boundaries of microcrack formation under compression by a complex of physical methods

Name of loading methods and types				Boundaries of microcrack formation	Values
Under compression	by the tensometric method (TM)	under cyclic loading	By average strains	R^v_{crc}/R_b	0.81
			By strains in the fracture zone	R^v_{crc}/R_b	0.75
			By maximum transverse and middle longitudinal strains	R^v_{crc}/R_b	0.35
		under monotonous loading	By average strains	R^0_{crc}/R_b	0.46
				R^v_{crc}/R_b	0.94
			By deformations in the fracture zone	R^0_{crc}/R_b	0.46
				R^v_{crc}/R_b	0.90
			By maximum transverse and average longitudinal strains	R^0_{crc}/R_b	0.23
				R^v_{crc}/R_b	0.75
	By ultrasonic pulse method (UPM)			R^0_{crc}/R_b	0.43
	By acoustic emission method (AEM)			R^0_{crc}/R_b	0.43
				R^v_{crc}/R_b	0.73
By tensometric method for tension on average strains				R^v_{crc}/R_b	0.75

Note: 150x150x600 mm prism specimens were tested at the age of 800 days.

The lower limit of microcrack formation R^0_{crc} of expanded clay concrete according to the tensometric method is weakly pronounced. It can be determined with a sufficiently large approximation only at the beginning of the increase in longitudinal and transverse strains (Figure 4) or with sufficient accuracy by acoustic emission and ultrasound [15].

The authors of the reference [9] conducted experimental studies of the operation of various types of concretes; as a result, new empirical dependencies were proposed to determine the boundaries of microcrack formation:

$$\eta^o_{crc} = R^o_{crc}/R_b = 0.33k_{crc} \times lnR_b - 0.15 \quad (4)$$

$$\eta^v_{crc} = R^v_{crc}/R_b = 0.33k_{crc} \times lnR_b + 0.1 \quad (5)$$

where R_b is the average strength of concrete, MPa; k_{crc} is the empirical coefficient.

Experimental data determined that there is a linear relationship between the values of relative loads for the upper and lower limits of microcrack formation [22]. The ratio of the values of the load level corresponding to the lower boundary of microcracking to the value of the load level corresponding to the upper boundary remains constant regardless of the class of concrete, i.e. $\eta^o_{crc}/\eta^v_{crc}$= const.

The value of ratio $\eta^o_{crc}/\eta^v_{crc}$ can be taken:

– $\eta^o_{crc}/\eta^v_{crc} \approx 0.67$ – for normal concrete [23];

– $\eta^o_{crc}/\eta^v_{crc} \approx 0.60$ – for expanded clay concrete [23];

The empirical coefficient k_{crc}, taken based on value k_{c1}, can be used when performing calculations for concrete and reinforced concrete structures:

$$k_{crc} = k_{c1} \times \eta^{o}_{crc}/\eta^{v}_{crc} \quad (6)$$

where $k_{c1} \approx 1.2$ – for expanded clay concrete with concrete density ρ < 2200 kg/m^3, and for other types of concretes $k_{c1} = 1.0$ with ρ > 2200 kg/m^3.

To determine the boundaries of microcrack formation in high-strength expanded clay concrete of a dense structure according to formulas (4 and 5), the values of numerical coefficients are determined by the least squares method based on the experimental data obtained by the authors

$$\eta^{o}_{crc} = R^{o}_{crc}/R_b = 0.21k_{crc} \times lnR_b - 0.11, \quad (7)$$

$$\eta^{v}_{crc} = R^{v}_{crc}/R_b = 0.21k_{crc} \times lnR_b + 0.21. \quad (8)$$

The average values of R^{o}_{crc} and R^{v}_{crc} obtained by the authors in the experiment for expanded clay concrete were compared with the values calculated using empirical formulas (proposed by Semenyuk S.D., Moskalkova Yu.G. (4, 5) [9, 24] and the authors of (7, 8)) (Table 7).

Table 7. Calculation results of relative values of microcrack boundaries

Concrete type	Average prism strength, $R_{cb.o}$ MPa	Values of ratio $\eta^{o}_{crc}/\eta^{v}_{crc}$		Relative values of microcrack formation boundaries				Deviations of calculated values from experimental ones, %	
		Test	Adopted	Test values		Values calculated according to formulas (4), (5)		According to the method of Semenyuk S.D. and Moskalkova Yu.G.	
				η^{o}_{crc}	η^{v}_{crc}	η^{o}_{crc}	η^{v}_{crc}	η^{o}_{crc}	η^{v}_{crc}
Normal concrete [9, 24]	22.3	0.667	0.67	0.54	0.81	0.536	0.786	0.4	2.4
	28.1	0.639	0.67	0.53	0.83	0.588	0.838	-5.8	-0.8
	28.2	0.679	0.67	0.57	0.84	0.588	0.838	-1.8	0.2
	29	0.674	0.67	0.58	0.86	0.595	0.845	-1.5	1.5
Expanded clay concrete [23]	15.9	0.667	0.60	0.50	0.75	0.507	0.757	-0.7	-0.7
	17.7	0.600	0.60	0.45	0.75	0.533	0.783	-8.3	-3.3
Authors' data according to formulas (7, 8)	35.7	0.57	0.60	0.43	0.75	0.431	0.751	-0.1	-0.1

The data given in Table 4 clearly demonstrate the adequacy of the application of the empirical formulas proposed by the authors in (7, 8) to determine the relative values of the boundaries of microcracking in high-strength expanded clay concrete of a dense structure.

3.2 Long-term strength of expanded clay concrete

On the graphs of Figure 6, the values of the level of long-term strength in semilogarithmic coordinates are plotted depending on the staying time of the specimens under load ($t–\tau_1$). At the same time, curves corresponding to dependence (3) were plotted. Figure 3 shows that for expanded clay concrete, there is a good agreement between the experimental data and the approximating dependence. The deviations of the experimental values of the level of

long-term strength from the values calculated by dependence (3) do not exceed 10%.

The relationship between the level of long-term strength and the time of staying of specimens under loading was taken as:

$$\eta = (t, \tau_1) = a - b \log(t - \tau_1), \qquad (9)$$

where $a = 0.868$ and $b = 0.032$ – the values under axial compression, and $a = 0.915$ and $b = 0.028$ are the values under axial tension, determined by the least squares method based on the experimental data obtained by the authors.

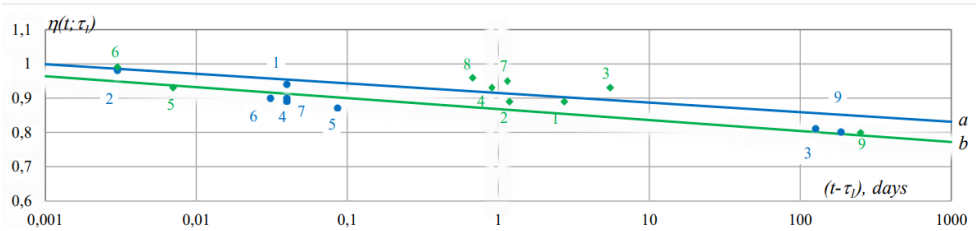

Fig. 9. Change in the long-term strength of expanded clay concrete over time under axial tension (a) and compression (b) by dependence (3)

3.3 Comparison of the boundaries of microcrack formation with the long-term strength of expanded clay concrete

A comparison of values of R^{v}_{crc}, determined by the tensometric method (TM) under cyclic and monotonic loading and by the acoustic emission method (AEM) with the limit of long-term compressive and tensile strength is given in Table 8.

Table 8. Comparison of the boundaries of microcrack formation of expanded clay concrete under compression and tension (R^{v}_{crc}/R_b and R^{v}_{crc}/R_{bt}) with the long-term strength (R_{bl}/R_b и R_{btl}/R_{bt})

Type of load					Value
Compression	$\frac{R^{v}_{crc}}{R_b}$	under cyclic loading	TM	by average strains	0.81
				by strains in the zone of destruction	0.74
		under monotonous loading	TM	by average strains	0.94
				by strains in the zone of destruction	0.90
			AEM		0.75
	R_{bl}/R_b				0.74
	$\frac{R^{v}_{crc}}{R_{bl}}$	under cyclic loading	TM	by average strains	1.09
				by strains in the zone of destruction	1.00
		under monotonous loading	TM	by average strains	1.27
				by strains in the zone of destruction	1.22
			AEM		0.99
Tension	$\frac{R^{v}_{crc}}{R_{bt}}$	under monotonous loading	TM		0.75
	R_{btl}/R_{bt}				0.79
	R^{v}_{crc}/R_{btl}				0.95

Analysis of the comparison results shows that for expanded clay concrete, the best comparison of the values of the limit of long-term strength R_{bl} and the upper limit of microcracking R^{ν}_{crc} under compression [22] gives the value of R^{ν}_{crc} The acoustic emission method and the tensometric method in the fracture zone under cyclic loading are determined. From this, it follows that to determine the long-term strength based on the results of short-term tests, it is recommended to test specimens with both monotonically increasing and cyclic loads with the unloading at each stage, measuring strains on loading and unloading in several sections (more than three) along the height of the specimen in the zone of a homogeneous stressed state. As the limit of the long-term strength of expanded clay concrete, we take the stress corresponding to the extremum on the diagram of the inelastic component of volumetric strain, determined from the measurement data of strains in the destruction zone as the difference between the total diagram ε_{ν} according to the results of monotonic loading and the elastic component ε^{e}_{ν} according to the results of cyclic loading. Or else, it is recommended to determine the value of R^{ν}_{crc} by the method of acoustic emission under monotonic loading.

A comparison of the values of the long-term strength and the upper limit of microcracking under axial tension (Table 8) shows that for expanded clay concrete, the values of R^{ν}_{crc} and R_{btl} correspond to each other (the discrepancy is no more than 13%).

4 Conclusions

1. It was determined that the ratio of R_{bt}/R was 0.05...0.06, and R_{bt}/R_b - 0.06...0.07, and the values of the initial Poisson's ratio of expanded clay concrete under compression and tension correspond to the values regulated by building standards in SNiP.

2. The results obtained indicate the best resistance of expanded clay concrete under low-cycle compression loading and the expediency of their use in the structures of transport facilities, where the structures are subject to multiple low-cycle loads.

3. It was determined that the values of R^{ν}_{crc}, calculated by different methods are in good agreement with each other, which cannot be said about R^{o}_{crc}. The values of R^{ν}_{crc}, obtained by the acoustic emission method are in good agreement with the values of R^{ν}_{crc}, obtained by the tensometric method in the fracture zone (the discrepancy is no more than 8%).

4. The statement confirmed that for expanded clay concrete, the values of relative levels of crack formation $\mathrm{R}^{0}_{crc}/\mathrm{R_b}$ and $\mathrm{R}^{\nu}_{crc}/\mathrm{R_b}$ are higher than traditional heavy concrete of the same strength.

5. An empirical formula appropriate for practical application was obtained for determining the boundaries of microcrack formation and describing the pattern of change in the long-term strength of expanded clay concrete under axial compression and tension; this formula allows (at the stage of projecting) considering the long-term strength for any time interval.

6. It was determined that for expanded clay concrete, the best comparison of the values of the long-term strength R_{bl} and the upper limit of microcrack formation R^{ν}_{crc} under compression gives the value of R^{ν}_{crc}, determined by the acoustic emission method and the tensometric method in the fracture zone under cyclic loading.

References

1. Raupov Ch., Shermukhamedov U., and Karimova A. Assessment of strength and deformation of lightweight concrete and its components under triaxial compression, taking into account the macrostructure of the material. In E3S Web of Conferences, **264**, p. 02015 (2021)

2. Raupov Ch., Karimova A., Zokirov F., and Khakimova Y. Experimental and theoretical assessment of the long-term strength of lightweight concrete and its components under compression and tension, taking into account the macrostructure of the material. In E3S Web of Conferences, **264**, p. 02024 (2021)
3. Raupov Ch.S. Expanded clay concrete for transport construction: Monograph, Tashkent: Tamaddun, p. 356 (2020)
4. Raupov Ch.S., Umarov Kh.K. Recommended areas of application of expanded clay concrete in bridge building and its effectiveness. Bulletin of TashIIT. **1**, pp. 6-9 (2010)
5. Ashrabov A.A., Raupov Ch.S. Work of lightweight concrete beams in view of a descending branch of the diagram. International Conference held in Malaysia, the collection of scientific researches, pp 139–142 (2002)
6. Ashrabov A.A., Raupov Ch.S. The normalization of long-lived durability of lightweight concrete at monoaxial stressing. International Conference held in Malaysia. The collection of scientific researches, pp 134–138 (2002)
7. Raupov Ch.S. Technology for the manufacture of bridge structures from high-strength expanded clay concrete. Bulletin of TashIIT. **2**, pp. 11–15 (2008)
8. Farhad Ansari. Mechanism of microcrack formation in concrete. ACI Materials Journal, **86**(5), pp. 459–464 (1989)
9. Semenyuk S.D., Moskalkova Yu.G. Methods for determining the boundaries of microcrack formation. Construction of unique buildings and structures, **7**(70). pp. 22-30 (2018) doi: 10.18720/CUBS.70.2
10. Chini A.R., Villavicencio E. J. Detection of Microcracks in Concrete Cured at Elevated Temperature. University of Florida, p. 86. Gainesville, (2006)
11. Thomas T. C. Hsu. Fatigue and microcracking of concrete. Materials and Structures. 17(1). pp. 51–54 (1984)
12. Camacho, E. J. V. Analysis of Microcrack Behavior in Mass Concrete. Doctoral dissertation, University of Florida (2006).
13. A. Ashrabov, C. S. Raupov, A. A. A. Samad, J. Jayaprakash. Stady on force transfer mechanizm in cracked reinforced concrete elements. The International Conference on problems of mechanics and seismodynamics of structures, pp. 28–31 (2004)
14. A. A. Ashrabov, Y.V. Zaitsev, S. Spotar, C. S. Raupov. Modelling and strength simulation for concrete materials containing cracks. Journal of Problems of Mechanics. № 4, pp. 11–17, Tashkent (2005)
15. Guchkin I.S. Study of the process of micro-destruction of expanded clay concrete under uniaxial compression by a complex of physical methods. p. 150, Penza (1973)
16. Golyshev A.B., Bachinsky V.Ya., Polishchuk V.P. Reinforced concrete structures, Strength of concrete. Kyiv (2001)
17. A. A. Ashrabov, M. S. Jaafar, W.A.M. Thanoon and C. S. Raupov. Static Fatigue Strength of Lightweight Concrete at Uniaxial Loading. Proceedings of the 2nd World Engineering Congress Sarawak. Structural engineering and construction anagement. Ingineering Innovation and Sustainability: Global Challenges and Issues. pp. 98–101 Malaysia (2002)
18. Moskalkova Yu. G. Strength and deformability of bent reinforced concrete elements, reinforced by the build-up of a compressed zone, under static and low-cycle loading: Belarusian-Russian University Mogilev, p. 199 (2013)
19. Semenyuk S.D., Moskalkova Yu.G. Strength and deformability of bent reinforced concrete elements reinforced by the growth of a compressed zone under static and low-

cycle loading. Monograph, Belarusian-Russian University Mogilev, p. 274 (2017)

20. Kalandarov K. Effect of cyclic loading on the work of eccentrically compressed reinforced concrete elements. p. 185, Samarkand (1994)
21. Khodzhaev A.A. Improving the calculation of reinforced concrete structures under regime loading. p. 437, Tashkent (1997)
22. Chini A.R., Villavicencio E. J. Detection of Microcracks in Concrete Cured at Elevated Temperature. University of Florida, p. 86 Gainesville, (2006)
23. Moskalkova Yu. H. Behavior of claydite at the stage of microcrack formation. Science and Construction, **3** (13), pp. 40 – 43. Kiev, (2017)
24. Semenyuk S. D., Moskalkova Yu. G. Strength and deformability of bent reinforced concrete elements reinforced by the build-up of a compressed zone under static and low-cycle loading: monograph. Belarusian-Russian University Mogilev, p. 274 (2017)